



SCHOOL OF STATISTICS
UNIVERSITY OF THE PHILIPPINES DILIMAN



WORKING PAPER SERIES

Control Chart for Monitoring Autocorrelated Process with Multiple Exogenous Inputs

by

Ma. Sofia Criselda A. Poblador
University of the Philippines Manila

Erniel B. Barrios
University of the Philippines Diliman

UPSS Working Paper No. 2014-01
January 2014

School of Statistics
Ramon Magsaysay Avenue
U.P. Diliman, Quezon City
Telefax: 928-08-81
Email: updstat@yahoo.com

Control Chart for Monitoring Autocorrelated Process with Multiple Exogenous Inputs

Ma. Sofia Criselda A. Poblador
University of the Philippines Manila

Erniel B. Barrios
University of the Philippines Diliman

Abstract

We propose to use AR-Sieve Bootstrap in the construction of a control chart of an autocorrelated process influenced by multiple exogenous inputs. The control charts are compared with EWMA control chart through a simulation study. AR-Sieve bootstrap control limits are narrower than EWMA control limits. While the proposed method yields a higher rate of false alarms, it is quick in detecting even minimal structural changes.

Keywords: AR-Sieve Bootstrap, control chart, model uncertainty, autocorrelated process, EWMA

1. Introduction

Monitoring of process performance is an essential element in ensuring that the product or service being offered meets the expectations of recipients/customers within a specific time frame. Control charts are important tools in monitoring variability and stability of processes. In manufacturing, engineers rely heavily on various control charts in detecting and resolving problems associated with the process. Control charts are also extensively used in healthcare and public health surveillance, e.g., in monitoring diseases and hospital performance. In business intelligence and data mining, companies have recently shown interest in using control charts as a tool in quality performance and monitoring. Different companies offering products or services have the same goal – to maintain high quality and achieve consistent performance in satisfying the customers.

The Shewhart control chart assumes that the process data constitute a set of independent and identically-distributed measurements. In many instances, process data are correlated, either temporally, spatially or due to nested sources of variation [1]. This correlation is usually caused by the high frequency of sampling due to the automated measurement and recording technology, with consecutive samples being similar in nature and hence statistically correlated [2]. For autocorrelated data, the performance of Shewhart control chart is markedly affected. Particularly, the number of observations until an out-of-control point is observed when the process is still in-control significantly decreases, which means that an in-control process is disrupted quicker when there is autocorrelation. False signals leading to abrupt interruptions in the operation may cause problems for some sectors and subsequently affecting quality and/or production efficiency.

In monitoring autocorrelated processes, an ARIMA model is fitted and the residuals are used in constructing the control limits. However, the order of the ARIMA model is a confounding issue since incorrect specification leads to inferior parameter estimates that will produce large residuals. The resulting control limits can be unusually wide and will have difficulty in detecting signals in the process.

Several nonparametric strategies in construction of control charts have thrived on recent literature, which basically involves simulation from an estimated distribution based on resamples. In particular, AR-Sieve bootstrap is a nonparametric procedure which addresses issues associated with residual-based methods such as model uncertainty and dependence on large samples. [3] used the AR-Sieve bootstrap in constructing a control chart based on residuals, with a very mild assumption that the true underlying process allows for an autoregressive representation of order infinity with Gaussian innovations. [4] used the same procedure in constructing control limits to monitor actual process observations, instead of residuals.

This paper complements the work of [4] in suggesting a procedure in addressing the issue of the adverse effects of model uncertainty in constructing a control chart to monitor actual process observations. We assume that the true underlying process, influenced by multiple input series through a stochastic-dynamic filter function allows for an autoregressive representation of order infinity with Weibull innovations. Prediction limits are constructed using the AR-Sieve bootstrap in plotting the original process data, ultimately mitigating the possible impact of model uncertainty owing to the application of a nonparametric design procedure.

As [4] observed, AR-Sieve bootstrap control chart provides a more acceptable in-control and out-of-control run lengths and lower false alarm rate than standard control chart designs in monitoring autocorrelated processes. The common problems of small sample size and model misspecification are addressed by the nonparametric procedure aforementioned. Residual-based control charts track the actual process observations by means of adjusted prediction limits, the latter approach is easily communicated during actual process monitoring.

Aside from naturally exhibiting some degree of autocorrelation, most real-life processes depends on several exogenous factors. This study proposes the use of a control chart in monitoring the behavior of an autocorrelated process, influenced by some external processes using the nonparametric methodology.

Credit risk, for instance, is an autocorrelated process that is highly dependent on several demographic and economic variables. In particular, the risk due to nonpayment of a loan may be influenced by the overall quantity of unsecured loans as well as the amount of new loans. Essentially, it is of main interest for banking institutions to discriminate between good customers and bad customers in terms of credit worthiness. Many conventional approaches are effectively useful in addressing this need. Additionally, it is also of utmost importance to maintain credit risk within an acceptable set of parameter limits. [5] were able to set two credit warning lines using modern corporate finance model as tool to monitor credit risk. Then

again, the structural Kealhofer-McQuown-Vasicek (KMV) model is prone to misspecification error and misleading predictive accuracy.

The idea of setting up credit warning lines to effectively monitor credit risk will be significantly enhanced by this study. The proposed nonparametric methodology in constructing prediction limits takes into account the problem of model uncertainty, thus, yields better performance in terms of run lengths and false alarm rate.

2. Control Charts

A control chart is a graphical display of process behavior, allowing for quick monitoring of process variability and detection of unusual process shifts. The two causes of process variation are (1) random/common and (2) nonrandom/assignable. The process is said to be in a state of statistical control when any variation is only a result of random inherent variability in the process. On the other hand, the process is said to have shifted significantly out-of-control once variation is induced by some nonrandom, assignable aspect associated with the process. Process stability is achieved as soon as successful distinction between these two causes of variation is made. While the process is in a state of statistical control, that is, variation in the process can only be attributed to random causes, lower and upper control limits are constructed, which are expected to contain measurements of a process that is in-control. Any observed measurement plotted outside these control limits is a realized value of the process that went beyond the expected variation of the process, and is most likely induced by a nonrandom, assignable cause of variation, which signals a possible shift in the process. A good understanding of variation in the process can effectively improve performance and reduce cost.

Let $\bar{X}_1, \bar{X}_2, \dots$ be a sequence of sample means of measurements of quality. Assume that the sample means are independent normal random variables with a common probability density function $f(x)$. Without loss of generality, the in-control process mean and standard error of the sample mean are assumed to be zero and one, respectively. A Shewhart control chart is obtained by plotting \bar{X}_t against the sample number t where $t = 0, 1, \dots$. An out-of-control signal is issued when $\bar{X}_t < L$ or $\bar{X}_t > U$, where L and U are commonly known as the lower and upper control limits. Shewhart control charts, however are unable to detect small process shifts quickly enough, [6].

The Exponentially-Weighted Moving Average (EWMA) control chart for detecting a change in the process mean was introduced by Roberts in 1959. At the t^{th} sample, the EWMA chart uses the control statistic $Y_t = (1 - \lambda)Y_{t-1} + \lambda\bar{X}_t$ where the starting value Y_0 is a constant y_0 , and $0 < \lambda \leq 1$ is a parameter of the control chart. There are thus two parameters to the EWMA chart, λ and h , where λ is a weighting constant which is in the range (0,1]. Small values of λ produce a chart which is sensitive to small shifts and large values of λ produce a chart

which is sensitive to large shifts. When $\lambda = 1$, the EWMA chart reduces to Shewhart \bar{X} - chart.

The chart signals a shift in the process mean when Y_t falls outside of control limits, given by $\mu \pm h\sigma_{\bar{x}}\sqrt{\frac{\lambda}{2-\lambda}}$ where $\sigma_{\bar{x}}\sqrt{\frac{\lambda}{2-\lambda}}$ is the asymptotic standard deviation of Y_t when the observations are independent.

The most known measure for evaluating the performance of a control chart is the average run length (ARL), which is expected number of observed measurements until an out-of-control signal is made based on the distribution of the run lengths. Run length is computed by counting the number of observations until an out-of-control signal is made. When the process is in-control, the ARL of a chart is ideally as large as possible so that the running process is not affected by frequent false out-of-control alarms, which are usually disruptive in nature. On the other hand, when the process is out-of-control, the ARL should be as small as possible so that any assignable cause of variation could be sought out and eliminated. The false alarm rate (FAR) is the probability that a control chart gives an out-of-control signal when in fact the process is still in-control.

3. Bootstrap Methods

Different bootstrap methods have been proposed in analyzing stationary time series data. A model-based approach which resamples from approximately identically and independently distributed residuals resolves the autocorrelation issue in time series data but is sensitive to model misspecification. Alternatively, a nonparametric, purely model-free bootstrap scheme for stationary observations, blockwise bootstrap resamples (overlapping blocks of consecutive observations) where the blocklength involved grows slowly with the sample size was proposed by [7]. The blockwise bootstrap benefits from robustness against misspecification. However, the resampled series ignored the dependence between different blocks, which result to nonstationary bootstrap samples. [8] makes use of the older idea of fitting parametric models first and then resampling from the residuals. But instead of considering a fixed finite-dimensional model, an infinite-dimensional, nonparametric model will be approximated by a sequence of finite-dimensional parametric models. This strategy is known as the method of sieves.

Assume that the process is in a state of statistical control and observations are generated by a stationary process, $\{Y_t\}_{t \in Z^+}$, which allows an autoregressive representation of order infinity,

$AR(\infty)$, i.e., $Y_t - \mu = \sum_{j=1}^{\infty} \phi_j(Y_{t-j} - \mu) + \varepsilon_t$, $t \in Z$, where $\mu = E(Y_t)$, ϕ_j 's are the parameters such that $\sum_j \phi_j^2 < \infty$ and ε_t is an iid innovation sequence following a Gaussian distribution with $E(\varepsilon_t) = 0$ and $Var(\varepsilon_t) = \sigma^2$, [3]. This representation motivates the $AR(\infty)$ -Sieve Bootstrap, proposed by [9] and [10], and extended by [11], [8] and [12] as cited by [13].

Following [8], the sieve algorithm proceeds as follows:

- (1) Get a sample from an in-control AR process $\{Y_t\}$.
- (2) Fit an AR(\hat{p}) model with increasing order \hat{p} as sample size increases. Estimate the order $\hat{p} = p(n)$ using the AICC criterion of [14] and [15]. The AICC is bias-corrected version of the AIC given by the formula $AICC = -n \log(\sigma^2) + \frac{2n(p+1)}{n-p-2}$ which counteracts the over-fitting nature of the AIC by assigning a more extreme penalty for large-order models. An advantage of using the AICC criterion is that it is less affected than other criteria by the changes in the maximum order considered. The value of the maximum order p_{\max} has virtually no effect on the model chosen while for many other criteria, increasing the value of p_{\max} leads to increased over-fitting of the model [13]. Also, this criterion is preferred because the true model can be complex and not of finite dimension.
- (3) Characterize the AR(\hat{p}) model by estimating its infinite-dimensional parameter vector denoted by $\underline{\beta} = (\mu, \sigma, \phi_1, \phi_2, \dots)$. The vector of estimates is given by $\underline{\hat{\beta}} = (\hat{\mu}, \hat{\sigma}, \hat{\phi}_1, \hat{\phi}_2, \dots)$.
- (4) Compute the residuals

$$e_t = \sum_{j=0}^{\hat{p}} \phi_j (Y_{t-j} - \hat{\mu}), \quad t \in \{\hat{p} + 1, \dots, n\} \quad \text{eq. 5}$$

where $\hat{\phi}_0 = 1$ and calculate their mean.

$$\bar{e}_t = (n - \hat{p})^{-1} \sum_{t=\hat{p}+1}^n e_t \quad \text{eq. 6}$$

Obtain the centered residuals

$$\tilde{e}_t = e_t - \bar{e}_t \quad \text{eq. 7}$$

and define the empirical distribution function of the centered residuals

$$F_{\tilde{e}_t}(x) = (n - \hat{p})^{-1} \sum_{t=\hat{p}+1}^n I_{\{\tilde{e}_t \leq x\}} \quad \text{eq. 8}$$

- (5) Draw a resample ε_t^* of $n - \hat{p}$ iid observations from $F_{\tilde{e}_t}$.
- (6) Generate independent bootstrap samples $\{Y_t^*\}$ by the recursion

$$\sum_{j=0}^{\hat{p}} \hat{\phi}_j (Y_{t-j}^* - \hat{\mu}) = \varepsilon_t^* \quad \text{eq. 9}$$

where the starting \hat{p} observations are equal to $\hat{\mu}$.

In order to obtain a pseudo-stationary in-control sequence Y_t^* , the resamples are generated using equation 9 with sample size equal to $n + 100$ and the first 100 observations are then discarded.

- (7) Consider any statistics $T_n = T_n(X_1, X_2, \dots, X_n)$ where T_n is a measurable function of n observations. By plug-in principle, the bootstrapped statistics are defined by $T_n^* = T_n(X_1^*, X_2^*, \dots, X_n^*)$.

3. Methodology

We propose a procedure in construction of a control chart for any linear, invertible process (autocorrelated). Without loss of generality, assume that through the AICC criterion, an approximate $AR(\hat{\rho})$ model is identified for the process.

Step 1. Fit a transfer function model to the series $\{Y_t\}$ and obtain an estimate of the parameters of the $AR(\hat{\rho})$ model and the transfer function coefficients.

Step 2. Compute the residuals $\{e_t\}$ from the fitted model and calculate the mean square error of the residuals to obtain an estimate of the error variance, $\hat{\sigma}^2$.

Step 3. Generate a resample $\{e_t^*\}$ from a particular distribution with mean zero and variance $\hat{\sigma}^2$.

Step 4. Generate the bootstrap sample $\{Y_t^*\}_{t \in -n, -n+1, \dots, 0, \dots, n}$ through the recursion

$$Y_t^* = \hat{Y}_t + e_t^* \quad \text{eq. 10}$$

where \hat{Y}_t is the forecasted value of the transfer function model from step 1. Discard Y_t^* for all $t \in [-n, 0)$ i.e., remove the first $n+1$ observations. This should help in initializing the time series data, i.e., the effect of starting values will be eliminated.

Step 5. Repeat steps 3 – 4 B times, where B is a large number, so that B independent replicates of reconstructed samples, $\{Y_t^*\}_b$, $b \in \{1, 2, \dots, B\}$ are generated.

The estimation procedure for the control chart limits of the original process observations $\{Y_t\}$ is based on prediction limits. A $(1-\alpha) \times 100\%$ prediction limit on the forecast at time $t+1$, \hat{Y}_{t+1} , is constructed to provide a measurement of the precision of the forecast. In parametric

estimation, the prediction limits are constructed by $\hat{Y}_{t+1} \pm z_{\alpha/2} \sqrt{1 + \sum_{j=1}^t \phi_j^2 \sigma_e^2}$ where σ_e^2 is

the variance of the error terms. A nonparametric equivalent of these prediction limits for future observations is constructed using the AR-Sieve Bootstrap procedure. The method is used to simulate a large number of identical and independent stochastic processes to facilitate the characterization of the empirical distribution function $F_t(\cdot)$ of $\{Y_t\}_{t \in \mathbb{Z}^+}$ and consequently to derive the prediction limits of $\{Y_{t+1}\}_{t \in \mathbb{Z}^+}$.

Through the plug-in principle, the sieve bootstrap-generated control chart limits for the process at time $t+1$ are the lower and upper prediction limits of the interval, $(\hat{F}_t^{*\alpha/2}, \hat{F}_t^{*1-\alpha/2})$, where $\hat{F}_t^*(\cdot)$ is the estimated empirical distribution of the bootstrap sample $\{Y_t^*\}_b$, $b \in \{1, 2, \dots, B\}$. Specifically, the prediction intervals are the corresponding percentiles of $\hat{F}_t^*(\cdot)$.

Step 6. Obtain the $(\alpha/2)^{th}$ and the $(1-\alpha/2)^{th}$ percentiles of the estimated empirical distribution $\hat{F}_t^*(\cdot)$. Repeat this step for all future observations. Set the lower and upper control limits of the observation at time $t+1$ to be $L_{t+1} = \hat{F}_t^{*\alpha/2}$ and $U_{t+1} = \hat{F}_t^{*1-\alpha/2}$, respectively.

4. Simulation Study

The simulation study starts with the generation of the input and output series along with the innovation process following a particular structure and autocorrelation behavior. Specifically, the following steps were implemented:

Step 1. Simulate AR(1) processes $\{X_{1t}\}$ and $\{X_{2t}\}$ with autocorrelation coefficients ϕ_{X_1} and ϕ_{X_2} , and length n such that

$$X_{1t} = \phi_{X_1} X_{1,t-1} + u_t \text{ and } X_{2t} = \phi_{X_2} X_{2,t-1} + v_t \quad \text{eq. 11}$$

for $t \in \{-n, -n+1, \dots, 0, \dots, n\}$. We arbitrarily assign $u_t, v_t \sim \text{Weibull}(2.5, 10)$.

Step 2. Given the transfer function coefficients $(\omega_{1,0}, \omega_{1,1}, \omega_{2,0}, \omega_{2,1})$ and series length n , compute Y_t from

$$Y_t = \mu + \rho Y_{t-1} + \omega_{1,0} X_{1t} - \omega_{1,1} X_{1,t-1} + \omega_{2,0} X_{2t} - \omega_{2,1} X_{2,t-1} + \varepsilon_t \quad \text{eq. 12}$$

for $t \in \{-n, -n+1, \dots, 0, \dots, n\}$.

We arbitrarily assign $\mu = 10$ and $\varepsilon_t \sim \text{Weibull}(2.5, 10)$.

The boundaries of the simulated processes are based on the conditions provided in Table 1.

Table 1. Process Conditions in the Simulation Study

Description	Process Conditions	Value
Stationarity of the exogenous input factors	ϕ_{X_1}	0.5 (stationary) 0.9 (near-nonstationary)
	ϕ_{X_2}	0.5 (stationary) 0.9 (near-nonstationary)
Stationarity of the dependent process	ρ	0.5 (stationary) 0.8 (near-nonstationary)
Series Length	n	30 (very short) 70 (short) 100 (average) 200 (long)
Correlation of the input factors with the dependent process	$\omega_{i,0}, i = 1, 2$	1
	$\omega_{i,1}, i = 1, 2$	0.1 (low)

		0.9 (high)
--	--	------------

To capture behavior of customers in the credit risk sector, errors of each process are considered as Weibull. A considerable amount of empirical evidence shows that the distribution of returns is fat-tailed with mild negative skewness. Mandelbrot (1963) and Fama (1965) used non-Gaussian distributions in finance, while Mittnik and Ratchev (1989) also considered the Weibull, Lognormal and Laplace as unconditional return distributions. The Weibull distribution is a special case of an extreme value distribution and the generalized gamma distribution. It is widely used in the fields of material science, engineering and finance.

Weibull distribution was also used as an error distribution in range data modelling (Chen, et.al., 2008) and trading duration models (Engle and Russell, 1998).

Step 3. Follow steps 1 – 6 detailed in Section 3 to construct the AR-Sieve prediction limits for each computed series $\{Y_t\}$. Assume $AR(1)$ transfer function model for simplicity. The number of bootstrap replicates chosen is $B = 200$.

The simulation study computes for the 0.135th and 99.865th percentiles of the B bootstrap samples for every time t . These prediction limits allow for 99.73% of the observations to fall within the prediction interval during an in-control operation.

The EWMA central line control chart is constructed with two steps as follows:

Step 1. Obtain the forecast values $\{\hat{Y}_t\}$ from the fitted transfer function model in Step 1 of Section 3.1 as well as their corresponding standard errors $\sigma_{\hat{Y}_t}$, for $t \in \{-n, -n+1, \dots, 0, \dots, n\}$.

Step 2. Compute the lower and upper prediction limits as $\hat{Y}_t - k\sigma_{\hat{Y}_t}$ and $\hat{Y}_t + k\sigma_{\hat{Y}_t}$ respectively, where k determines the spread of the coverage of the prediction interval.

The EWMA central line control chart plots the forecasts from the fitted model as the central line of the control chart and it uses the standard errors of prediction to determine upper and lower control limits. The simulation study uses $k = 3$ in the construction of the EWMA control limits for every time t . This makes the width of the EWMA prediction interval similar to that of AR-Sieve.

Assessment of AR-Sieve Bootstrap Control Chart

Evaluation of the performance of the proposed nonparametric AR-Sieve Bootstrap control chart vis-à-vis EWMA is done using the following measures:

- (1) In-Control Run Length (IC RL). This is defined as the number of observations until a false alarm is signaled by the control chart, that is, an out-of-control point is detected while the process is still in-control. Ideally, the value of IC RL must be large to avoid erroneous interruptions during an in-control process.

(2) Out-of-Control Run Length (OC RL). This is defined as the number of observations until a correct alarm is signaled by the control chart, that is, an out-of-control point is detected when the process is already out-of-control. Preferably, the value of OC RL must be small enough for quick detection of process shift when the process has indeed shifted.

False Alarm Rate (FAR). This is defined as the proportion of points with respect to the length of the series or sample size, n , that incorrectly falls outside of the control limits. These occurrences are also referred to as ‘false signals’.

The following steps are undertaken for each computed series $\{Y_t\}$ to compute the evaluation measures of the control chart as defined above:

Step 1. Determine the false alarm rate (FAR) by observing the proportion of points that goes beyond all pairs of control limits (L, U) .

Step 2. Determine the IC run length by counting the number of points from the 1st observation value until the first OC point is signaled.

A crucial part in the simulation methodology is the replacement of the last 10% of the output series $\{Y_t\}$ with another set of observations generated as in Equation 12, only using a shifted value of ρ . The shift includes +0.02, +0.08, +0.1, +0.19 of the original values of ρ as specified in Table 1. The shifted series $\{Y_t^s\}_{t \in -n, -n+1, \dots, 0, \dots, n}$ is then used in applying steps 1 – 6 as detailed in Section 3.1 for the construction of the AR-Sieve prediction limits.

To evaluate the performance of a control chart in detecting an out-of-control condition, the final step proceeds:

Step 3. Determine the OC run length by counting the number of points from $(0.9n + 1)^{th}$ observation until the first OC point is signaled.

Structural change is introduced to the last 10% of the series to assess the impact of the shift it would cause on the process and how these can be detected by the control charts. The measures of IC RL, OC RL and FAR are then computed for the proposed method vis-à-vis EWMA.

5. Results and Discussion

Prediction limits are constructed using the nonparametric AR-Sieve Bootstrap for dependent processes given by

$$Y_t = 10 + \rho Y_{t-1} + X_{1t} - \omega_{11} X_{1,t-1} + X_{2t} - \omega_{21} X_{2,t-1} + \varepsilon_t$$

In particular, the lower and upper control limits for the $(t + 1)^{th}$ observation are generated by computing the 0.135th and 99.865th percentiles of the bootstrap samples at time t ,

respectively. As simulated, the dependent process $\{Y_t\}$ is affected by two exogenous factors, $\{X_{1t}\}$ and $\{X_{2t}\}$, so that equation 11 holds.

The simulation study is divided into six main settings, summarized in Table 2.

Table 2. Simulation Settings based on the Nature of Exogenous Inputs

SETTING	X1	X2	
1	stationary	stationary	independent
2	stationary	near-nonstationary	independent
3	near-nonstationary	stationary	independent
4	near-nonstationary	near-nonstationary	independent
5	stationary	stationary	correlated
6	near-nonstationary	near-nonstationary	correlated

The first setting consider stationary and independent exogenous inputs, X_1 and X_2 . Setting 2 consider one stationary and the other is near-nonstationary input but are independent. Setting 4 considers both exogenous inputs as near-nonstationary and still independent of each other. The remaining two settings consider the case when the exogenous inputs are correlated.

Further scenarios on other aspects of the model are generated under all possible combinations of process conditions, as presented in Table 3.

Table 3. Simulation Settings based on Process Conditions

Length of Series		Stationarity of Dependent Series		Correlation of the Inputs with Y			
n	Series Type	ρ	Stationarity	X1		X2	
n=30	Very Short	$\rho = 0.5$	Stationary				
n=70	Short	$\rho = 0.8$	Near-nonstationary	$\omega_{1,1} = 0.1$	Low	$\omega_{2,1} = 0.1$	Low
n=100	Average			$\omega_{1,1} = 0.9$	High	$\omega_{2,1} = 0.9$	High
n=200	Long						

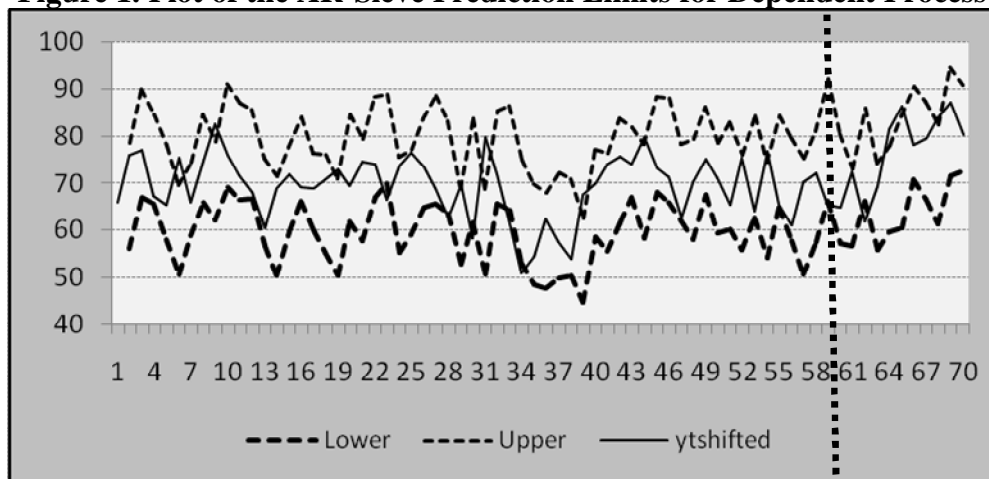
Moreover, sieve control limits are constructed for dependent processes with structural change in the last 10% of the data series. A structural change of +0.02 signifies that the last 10% of the data series, generated from a stationary dependent process (i.e., $\rho = 0.5$), are to be replaced with observations from another dependent process whose AR parameter is now 0.52. This is to test the sensitivity of the sieve control limits in detecting presence of true structural change in the data-generating process. Table 4 gives the various degrees of structural change introduced in each scenario, and their description.

Table 4. Process Mean Shift

Degree of Process Mean Shift	
+0.0	None
+0.02	Negligible
+0.08	Small
+0.1	Moderate
+0.19	Significant

As an illustration, Figure 1 presents an AR-Sieve control chart for a dependent process generated under Setting 1, whose process conditions are specified in the footnote of the chart.

Figure 1. Plot of the AR-Sieve Prediction Limits for Dependent Process



Setting 1: (i) $n=70$ (ii) Stationary dependent process (iii) Low correlation of past values of X_1 and X_2 with the dependent process (iv) +0.19 Structural Change

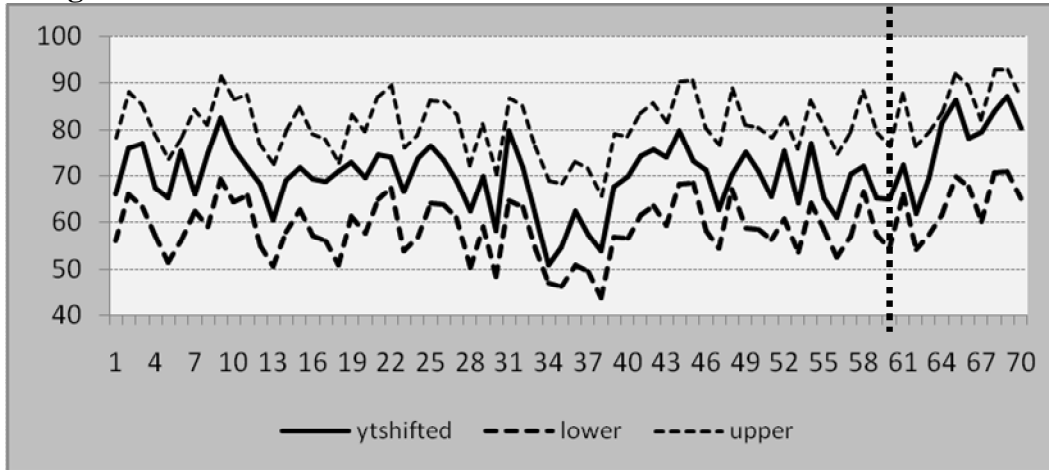
The solid line represents the actual observations generated from the dependent process. The lowermost and topmost line graphs denote the lower and upper sieve control limits, respectively. It can be noticed that the process exceeds the sieve limits as early as the 6th observation (IC RL=6). The false alarm rate is 24.64% while the in-control false alarm rate is 24.19%.

The vertical dashed line on the far right side of the control chart signifies a structural change of an amount of +0.19 in the last 10% of the process observations. On the 64th observation,

the control chart signals an alarm (OC RL=0), which indicates that the AR-Sieve control chart is immediately able to detect a shift in the process mean.

In comparison with EWMA Central Line Control Chart in Figure 2, where the lowermost and topmost line graphs represent the lower and upper EWMA control limits respectively, it can be seen that the solid line does not exceed the EWMA control limits all throughout the process (IC RL=None Detected). As a consequence, both false alarm rate and in-control false alarm rate are 0%. This implies that the EWMA Central Line Control Chart is insensitive to out-of-control points.

Figure 2. Plot of the EWMA Central Line Control Chart for the Process



Setting 1: (i) $n=70$ (ii) Stationary dependent process (iii) Low correlation of past values of X_1 and X_2 with the dependent process (iv) $+0.19$ Structural Change

Moreover, the EWMA control limits are not able to detect the structural change in the last 10% of the data series (OC RL=None Detected). This is due to the behavior of the EWMA control chart, when modified to deal with the problem of autocorrelation. The limits become wider, therefore less sensitive to out-of-control points resulting to slower detection of process shifts.

Finally, though AR-Sieve control limits appear to be narrower than the EWMA control limits, both are expected to contain 99.73% of the process observations when the process is in-control.

Effect of Series Length

We considered four series lengths in the simulation study summarized in Table 3. Holding the effect of the behavior of the exogenous inputs on the output process and other process conditions, the average IC RL, OC RL and FAR are computed within each series length and summarized in Table 5.

Table 5. Average IC RL, OC RL, and FAR of AR-Sieve and EWMA (by Length of the Series)

	Length of Series							
	n=30		n=70		n=100		n=200	
	Sieve	EWMA	Sieve	EWMA	Sieve	EWMA	Sieve	EWMA
IC RL	6.08	28.03	6.21	53.90	5.67	77.94	5.22	136.32
OC RL	0.61	0.19	1.45	0.55	1.43	0.77	3.04	3.38
FAR	0.20	0.01	0.22	0.01	0.23	0.01	0.23	0.01

As sample size increases, the average number of observations until false alarm detection (IC RL) is consistently 5 to 6 observations for AR-Sieve and increasing for EWMA. Due to narrower limits, AR-Sieve tends to detect disruption in the output process much earlier than EWMA, regardless of the length of the series.

Moreover, it can be seen from Figure 3 that AR-Sieve yields more or less the same IC RL (median IC RL is between 5 to 6) regardless of sample size, with 75% of scenarios having IC RL values less than 10. Few scenarios are plotted as outliers, with IC RL values ranging from 15 to 30 across the four sample sizes.

Relative to the average number of observations until correct alarm detection (OC RL), the results are not quite the same. As sample size increases, both AR-Sieve and EWMA yield increasing average OC RL values.

Figure 3. Box Plots of IC RL of AR-Sieve Control Limits across Series Lengths

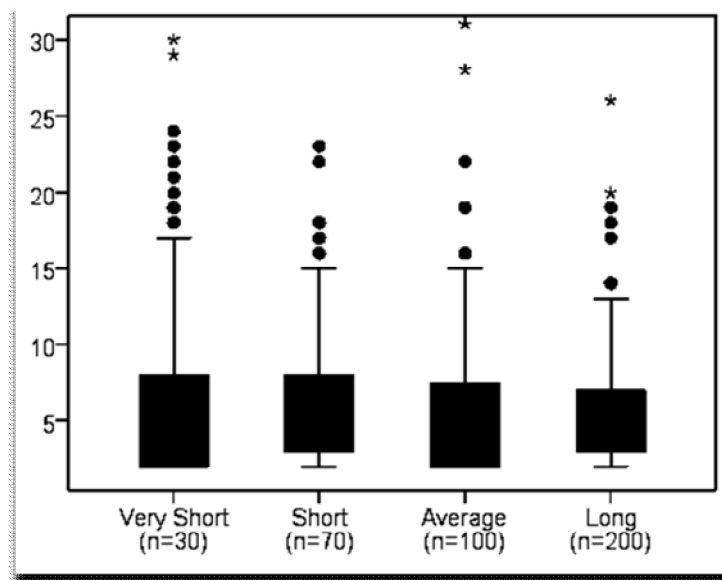


Figure 4. Box Plots of OC RL of AR-Sieve Control Limits across Series Lengths

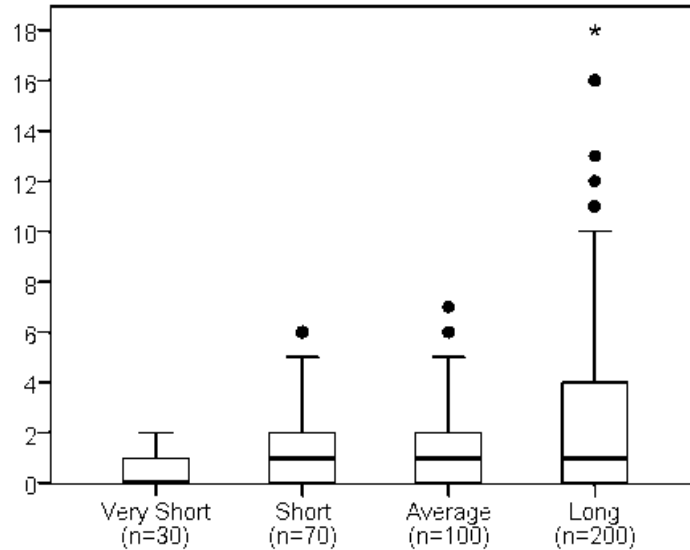
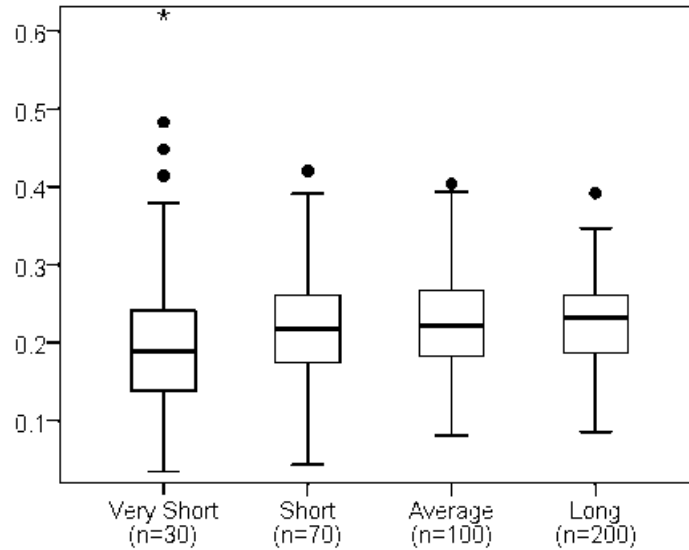


Figure 4 shows the empirical distribution of OC RL values of AR-Sieve control limits for simulated scenarios across different sample size. As series length gets longer, the distribution of OC RL evidently becomes more positively skewed. Median OC RL increases in proportional to sample size, with value close to 0 for very short series and around 1 for the remaining series lengths. AR-Sieve yields desirably very small OC RL values (between 0 and 2) for all scenarios under very short series. While 75% of scenarios with both short and average sample size have OC RL values less than 2, 75% of scenarios with long data series have OC RL values less than 4. Outlying scenarios with long data series have OC RL values ranging from 10 to 20.

Finally, Figure 5 shows the behavior of the false alarm rates FAR is not affected by sample size, consistently, median value around 20%. Moreover, three-fourths of all scenarios across four different series lengths have FAR less than 25%. However, the distribution of FAR is more variable in shorter series lengths with outlying values ranging from 40% to 60%.

Figure 5. Box Plots of FAR of AR-Sieve Control Limits across Series Lengths



Though EWMA has larger average IC RL and smaller average OC RL and FAR compared to the average values of AR-Sieve, it has an alarmingly high percentage of non-detection of in-control alarms and worse, out-of-control alarms.

It can be seen from Table 6 that AR-Sieve is able to detect in-control alarms for all scenarios with different series lengths (0% non-detection). On the other hand, EWMA is not able to detect in-control alarms for 87.5% of scenarios with very short data. However, as sample size increases, the percentage of non-detection of in-control alarms of EWMA clearly decreases, but remains high. This means that EWMA is mostly inclined to consider a process to be continuously in-control, in as much as not signaling false alarms during the entire operation of most processes.

Table 6. Percentage of Non-detected Alarm Points (by Length of the Series)

	Length of Series							
	n=30		n=70		n=100		n=200	
	Sieve	EWMA	Sieve	EWMA	Sieve	EWMA	Sieve	EWMA
IC Alarm	0.0	87.5	0.0	70.4	0.0	62.9	0.0	47.5
OC Alarm	28.8	91.3	14.6	81.7	2.9	85.4	0.8	79.2

Out-of-control alarms are most likely to remain undetected for scenarios with very short data, with 28.8% non-detection under AR-Sieve versus 91.3% non-detection under EWMA. This means that AR-Sieve cannot detect structural change for 29 out of 100 processes with very short data; likewise, EWMA cannot detect structural change for 91 out of 100 processes with very short data.

It can be observed that the percentage of non-detection of out-of-control alarms is inversely proportional to sample size. Nevertheless, the difference in the percentage of non-detection of

out-of-control alarms between AR-Sieve and EWMA is large. Particularly for long data series, the percentage of non-detection of out-of-control alarms under AR-Sieve reduced to 0.8%, while under EWMA declined only up to 79.2% of total scenarios with long data series. In other words, AR-Sieve cannot detect structural change for only 1 out of 100 processes with long data; while EWMA cannot detect structural change for 72 out of 100 processes with long data.

The proposed methodology is robust to sample size based on IC, RL, and FAR, whereas, OC and RL increases in proportion to sample size. The percentage of non-detection of out-of-control alarms decreases as series length increases.

Effect of the Correlation of Exogenous Inputs with the Output Process

The performance of AR-Sieve control limits is also assessed vis-à-vis EWMA control limits relative to the correlation of the exogenous inputs with the dependent output process. Four possible combinations of the levels of correlation of two exogenous inputs, X_1 and X_2 , with the dependent output process Y are presented as major columns in Table 7. The results are similar across series lengths. When both inputs have high correlation with the output, the average IC RL and OC RL are lower and the average FAR is higher compared when the correlation is low. This means that when both exogenous inputs are highly correlated with the output process, the AR-Sieve control limits are most likely to cause earlier disruption in the process, quicker detection of structural change and higher rate of false alarm. EWMA control limits do not quite exhibit the same behavior.

Table 7. Average IC RL, OC RL, and FAR of AR-Sieve and EWMA (by Correlation of Inputs with Output and Length of the Series)

		Correlation of X1 and X2 with Y							
		Low, Low		Low, High		High, Low		High, High	
		Sieve	EWMA	Sieve	EWMA	Sieve	EWMA	Sieve	EWMA
IC RL	30	7.08	29.29	5.70	28.00	6.50	24.67	5.02	29.50
	70	8.23	53.00	5.92	49.70	5.67	59.32	5.02	53.56
	100	7.02	78.65	6.10	79.17	4.72	78.89	4.83	74.86
	200	5.67	122.58	5.15	137.56	5.67	132.66	4.40	158.31
OC RL	30	0.58	0.50	0.59	0.00	0.70	0.14	0.55	0.25
	70	1.44	0.69	1.67	0.44	1.19	0.42	1.50	0.60
	100	1.95	1.00	1.24	1.36	1.44	0.00	1.13	0.50
	200	3.83	2.08	3.00	1.75	3.10	5.38	2.23	3.53
FAR	30	0.15	0.01	0.19	0.01	0.20	0.00	0.26	0.01
	70	0.17	0.01	0.24	0.01	0.21	0.01	0.26	0.01
	100	0.17	0.01	0.23	0.01	0.22	0.01	0.28	0.01
	200	0.17	0.01	0.23	0.01	0.22	0.01	0.27	0.01

The percentages of non-detection of both in-control and out-of-control alarms across series length relative to the correlation of the exogenous inputs with the dependent output process are presented in Table 8. There is a notable difference on the percentage of non-detection of structural change by AR-Sieve when both exogenous inputs are either highly or poorly correlated with the output. Except for very short series, it appears that the percentage of non-detection of out-of-control alarms is lower when both exogenous inputs have high correlation with the output process. This means that AR-Sieve is able to detect structural change mostly in processes where exogenous inputs are highly correlated with the output than in processes where the correlation between input and output is low.

Table 8. Percentage of Non-detected Alarm Points (by Correlation of Inputs to Output and Length of the Series)

		Correlation of X1 and X2 with Y							
	n	Low, Low		Low, High		High, Low		High, High	
		Sieve	EWMA	Sieve	EWMA	Sieve	EWMA	Sieve	EWMA
IC Alarm	30	0.0	88.3	0.0	85.0	0.0	90.0	0.0	86.7
	70	0.0	76.7	0.0	66.7	0.0	68.3	0.0	70.0
	100	0.0	56.7	0.0	60.0	0.0	70.0	0.0	65.0
	200	0.0	40.0	0.0	46.7	0.0	46.7	0.0	56.7
OC Alarm	30	28.3	93.3	26.7	90.0	26.7	88.3	33.3	93.3
	70	28.3	78.3	10.0	85.0	13.3	80.0	6.7	83.3
	100	5.0	88.3	1.7	81.7	5.0	88.3	0.0	83.3
	200	1.7	80.0	1.7	86.7	0.0	78.3	0.0	71.7

Effect of Near-nonstationarity of the Output Process

Aside from its dependence on exogenous inputs, the output process is also affected by its own past values. The extent of its reliance on past values is characterized by its near-nonstationarity. If past values of the output process have minimal effect (close to 0) on the present value then the output process is stationary, otherwise if past values have dominating effect (near 1) on the present value then the output process is near-nonstationary. The marginal effect of the near-nonstationarity of the dependent output process on the performance of AR-Sieve control limits vis-à-vis EWMA is summarized in Table 9.

It can be observed that the average IC RL of AR-Sieve is lower for stationary output process with series lengths $n=30$ and $n=70$. Near-nonstationary output process has lower average IC RL under AR-Sieve with series lengths $n=100$ and $n=200$. This means that for shorter series, AR-Sieve causes an earlier interruption in dependent processes that do not rely heavily on their own past values. For longer series, AR-Sieve gives an early signal of false alarm in output processes which are highly affected by their own past values. EWMA, on the other hand, has higher average IC RL for near-nonstationary output processes across all series lengths.

Table 9. Average IC RL, OC RL, and FAR of AR-Sieve and EWMA (by Nature of Stationarity and Length of the Series)

	n	Nature of Stationarity of Y			
		Stationary		Near-nonstationary	
		Sieve	EWMA	Sieve	EWMA
IC RL	30	5.07	15.50	7.08	28.93
	70	5.83	30.40	6.58	60.20
	100	5.71	47.17	5.63	88.67
	200	5.28	104.18	5.17	150.72
OC RL	30	0.76	1.00	0.47	0.00
	70	1.37	1.29	1.53	0.20
	100	1.58	3.00	1.29	0.21
	200	3.51	7.68	2.56	0.74
FAR	30	0.22	0.00	0.18	0.01
	70	0.22	0.00	0.22	0.02
	100	0.23	0.00	0.22	0.02
	200	0.22	0.00	0.23	0.02

It can also be observed that both AR-Sieve and EWMA have lower average OC RL for near-nonstationary output processes. But the average FAR seems to be comparable between stationary and near-nonstationary output processes. This means that structural change can be quickly detected in output processes which highly depend on their own past values. While AR-Sieve yields higher rate of false alarms across series lengths, regardless of the near-nonstationarity of the output process, it cannot be deemed inferior to EWMA. Table 10 shows why AR-Sieve is better than EWMA relative to the percentage of non-detection of alarm signals during process operation.

**Table 10. Percentage of Non-detected Alarm Points
(by Nature of Stationarity and Length of the Series)**

	n	Nature of Stationarity of Y			
		Stationary		Near-nonstationary	
		Sieve	EWMA	Sieve	EWMA
IC Alarm	30	0.0	98.3	0.0	76.7
	70	0.0	87.5	0.0	53.3
	100	0.0	80.8	0.0	45.0
	200	0.0	67.5	0.0	27.5
OC Alarm	30	31.7	96.7	25.8	85.8
	70	18.3	88.3	10.8	75.0

	100	1.7	94.2	4.2	76.7
	200	0.0	84.2	1.7	74.2

AR-Sieve is able to detect false alarm signals in both stationary and near-nonstationary output processes at least once. On the contrary, EWMA yields very high percentage of non-detection of in-control alarms, which apparently decreases as sample size increases. Moreover, a lower percentage of non-detection of in-control alarms can be observed for near-nonstationary processes.

An out-of-control condition is most likely detected by both AR-Sieve and EWMA in near-nonstationary processes. This is the implication of observing lower percentage of non-detection of out-of-control alarms for near-nonstationary processes. Comparing the two control charts, it can be noted that the large difference highly favors AR-Sieve. As mentioned many times before, the percentage of non-detection of structural change decreases as sample size increases.

Effect of the Degree of Structural Change

The performance of AR-Sieve vis-à-vis EWMA is assessed by taking into account the effect of the extent of structural change. The simulation study shows that AR-Sieve has lower average IC RL than EWMA across series lengths and across different degrees of structural change, as presented in Table 11.

**Table 11. Average IC RL, OC RL, and FAR of AR-Sieve and EWMA
(by Degree of Structural Change and Length of the Series)**

		Structural Change									
		+0		+0.02		+0.08		+0.1		+0.19	
		Sieve	EWMA	Sieve	EWMA	Sieve	EWMA	Sieve	EWMA	Sieve	EWMA
IC RL	30	5.19	--	6.10	1.00	6.26	35.50	5.92	26.50	6.98	29.35
	70	5.96	19.67	5.50	35.00	6.63	62.14	6.25	67.25	6.88	58.79
	100	4.65	49.90	5.15	47.14	6.10	88.00	7.23	86.56	5.08	83.04
	200	5.46	105.60	5.31	113.41	4.71	148.85	4.77	160.11	5.63	140.73
OC RL	30	0.82	--	0.76	--	0.69	0.40	0.51	0.00	0.40	0.12
	70	1.71	3.00	2.50	--	1.17	1.20	1.18	0.38	0.73	0.41
	100	1.95	3.00	1.70	0.00	2.32	3.33	1.13	1.25	0.40	0.25
	200	4.40	7.50	4.19	8.50	2.68	4.00	2.81	3.78	1.04	2.64
FAR	30	0.21	0.00	0.20	0.00	0.21	0.00	0.19	0.00	0.19	0.02
	70	0.22	0.00	0.23	0.00	0.22	0.01	0.22	0.01	0.22	0.04
	100	0.22	0.00	0.23	0.00	0.23	0.01	0.22	0.01	0.23	0.04
	200	0.21	0.00	0.22	0.00	0.24	0.01	0.23	0.01	0.23	0.04

Regardless of the amount of structural change present in the output process across different series lengths, AR-Sieve tends to signal false alarm much earlier in the process. Moreover, the average FAR does not seem affected by the amount of structural change present in the output

process. Though AR-Sieve has higher false alarm rate than EWMA, nevertheless, the average OC RL of AR-Sieve is lower than EWMA. This means that the proposed method is able to detect any amount of structural change more quickly than EWMA. As already pointed out before, it can be noticed that the average OC RL increases in proportion to series length. But this increasing pattern in the average OC RL does not suggest a slower detection of structural change for longer data series. In fact, the ratio of average OC RL to sample size yields similar values across all series lengths.

Table 12 presents the percentage of non-detection of alarm signals across different amount of structural change and series lengths. As beforehand, AR-Sieve yields 0% non-detection of in-control alarms, which means that a false alarm is signaled at least once in the output process irrespective of the amount of structural change present and the sample size.

**Table 12. Percentage of Non-detected Alarm Points
(by Degree of Structural Change and Length of the Series)**

	n	Structural Change									
		+0		+0.02		+0.08		+0.1		+0.19	
		Sieve	EWMA	Sieve	EWMA	Sieve	EWMA	Sieve	EWMA	Sieve	EWMA
IC Alarm	30	0.0	100.0	0.0	97.9	0.0	95.8	0.0	91.7	0.0	52.1
	70	0.0	87.5	0.0	83.3	0.0	72.9	0.0	66.7	0.0	41.7
	100	0.0	79.2	0.0	85.4	0.0	60.4	0.0	47.9	0.0	41.7
	200	0.0	58.3	0.0	64.6	0.0	39.6	0.0	43.8	0.0	31.3
OC Alarm	30	41.7	100.0	29.2	100.0	25.0	89.6	27.1	97.9	12.5	64.6
	70	20.8	97.9	12.5	100.0	12.5	89.6	16.7	83.3	8.3	39.6
	100	8.3	95.8	2.1	97.9	2.1	93.8	0.0	91.7	2.1	50.0
	200	2.1	95.8	0.0	95.8	14.6	91.7	0.0	81.3	0.0	31.3

In comparison with the benchmark control limits, it can be seen that EWMA does not signal a false alarm in all output processes with +0 structural change and n=30. As structural change and series length increase, the percentage of non-detection by EWMA decreases, but remains ominously high. Moreover, it can be concluded from Table 12 that AR-Sieve has lower percentage of non-detection of out-of-control alarms than EWMA. As structural change and series length increase, the percentage of non-detection of out-of-control alarms by both control charts decreases. Particularly, this means that the control charts can detect a +0.19 structural change more quickly than a +0.02 structural change. Given these results, AR-Sieve is more likely to detect an out-of-control condition in most processes than EWMA.

Any amount of structural change is quickly detected by AR-Sieve than EWMA, in particular, when sample size is large, i.e., n=100 and n=200. Even when sample size is small, i.e., n=30 and n=70, AR-Sieve can still detect any amount of structural change in most output processes more quickly than EWMA.

6. Conclusions

A nonparametric AR-Sieve bootstrap control chart is proposed to monitor actual observations of a dependent process with multiple exogenous input factors. Results of the simulation study shows that the proposed methodology produces narrow control limits, making the

nonparametric control chart very sensitive to any degree of structural change. In general, shorter in-control (IC) and out-of-control (OC) run lengths (RL) are observed across independent scenarios of varied process conditions, indicating an early process disruption but quick detection of process shift, respectively. Similar results are obtained considering the effects of series length, the behavior of the exogenous inputs, correlation of the inputs with the output process, near-nonstationarity of the dependent output process and degree of structural change.

In particular, the average IC RL and FAR are not affected by varying series lengths, while the average OC RL is found to increase in proportion to sample size. Nevertheless, the increasing pattern in the average values of OC RL does not imply a slower detection of structural change. This is because the ratio of average OC RL to series length yields approximately similar values across different series lengths. Moreover, AR-Sieve gives a false alarm signal at least once during the entire process while an out-of-control condition is more likely to be detected for output processes with larger sample size.

AR-Sieve is robust to the behavior of the exogenous inputs. Meanwhile, the proposed method is able to detect structural change mostly in processes where exogenous inputs are highly correlated with the output than in processes where the correlation between input and output is low. Likewise, an out-of-control condition is more likely detected in near-nonstationary output processes. A larger amount of structural change is more easily detected, but even so, the AR-Sieve is still able to detect minimal amount of structural change.

In addition, the proposed methodology is evaluated vis-à-vis a benchmark control chart, designed to handle autocorrelation, which is the EWMA Central Line Control Chart. With the same confidence, EWMA generally produces larger in-control and out-of-control run lengths. Respective implications are a much delayed process disruption as well as a slower detection of structural change. Though EWMA, in general, has smaller false alarm rate, it cannot detect false alarm signals, more importantly, it remains insensitive to structural change in most output processes. Its wide control limits cause it to lean towards the dangerous assumption that the process is constantly in-control, to the extent of not being able to detect structural change during the entire operation.

When percentage of non-detection of out-of-control alarms is high, it means that the control limits are not able to give correct signals of an out-of-control condition in most processes. The consequence of such performance is detrimental, in that, the control chart views most processes as still operating in-control when in fact the routine is already broken which ultimately forfeits the goal of process monitoring.

Costs entailing non-detection of process shift is much higher than that of early process disruption. Advanced business strategies are necessitated by an early process disruption, making it more beneficial than disadvantageous.

References

1. Vander Wiel, S.A. Monitoring processes that wander using integrated moving average models. *Technometrics* 1995;**38**: 139–151.
2. Basawa, I.V., Lund, R., and Padgett, W.J.. A control chart for processes with correlated subgroups. *Technical Report No. 184*1996; Dept. of Statistics, Univ. of South Carolina.
3. Capizzi, G., and Masarotto, G. Bootstrap-based design of residual control charts. *IIE Transactions* 2008;**41**: 275-286.
4. Mancenido, M., and Barrios, E. An AR-sieve bootstrap control chart for autocorrelated process data. *Quality and Reliability Engineering International* 2012; **28**: 387-395 DOI: 10.1002/qre.1253.
5. Chen, X., Wang, X., and Wu, D. Credit Risk Measurement and Early Warning of SMEs: An Empirical Study of Listed SMEs in China. *Decision Support Systems*, 2010; **49**: 301-310.
6. Gan, F. Exponentially-weighted moving average control charts with reflecting boundaries. *Journal of Statistical Computation and Simulation* 1992; **46**: 45-67.
7. Künsch, H. The jackknife and the bootstrap for general stationary observations. *The Annals of Statistics* 1989;**17**: 1217-1241.
8. Buhlmann, P. Sieve bootstrap for time series. *Bernoulli: Official Journal of the Bernoulli Society for Mathematical Statistics and Probability* 1997;**3**:123-148.
9. Kreiss, J. P. Asymptotic statistical inference for a class of stochastic processes. *Habilitationsschrift* 1988; Universita't Hamburg.
10. Kreiss, J. P. Bootstrap procedures for AR(1)-processes. In *Bootstrapping and Related Techniques*, Jo'ckel, K., Rothe, G., and Sender, W., (eds). Springer-Verlag: Berlin, 1992:107-113.
11. Paparoditis, E. Bootstrapping autoregressive and moving average parameter estimates of infinite order vector autoregressive processes. *Journal of Multivariate Analysis* 1996; **57**: 277-296.
12. Inoue, A. and Kilian, L. Bootstrapping smooth functions of slope parameters and innovations variance in VAR(1) models. *International Economic Review* 2002; **43**: 309-331.
13. Alonso, A., Pena, D. and Romo, J. Introducing model uncertainty in time series bootstrap. *Statistica Sinica* 2004;**14**: 155-174.
14. Hurvich, C.M. and Tsai, C.L. Regression and time series model selection in small samples. *Biometrika* 1989;**76**: 297-307.
15. Hurvich, C.M. and Tsai, C.L. Bias of the corrected AIC criterion for underfitted regression and time series models. *Biometrika* 1991;**78**:499-509.